

Study On Pollution Performance on a Wind Turbine Blade Using OES Technique for Lightning and Switching Impulse Voltage Profiles

V. Sathiesh Kumar^{a*}, Nilesh J. Vasa^a, R. Sarathi^b

^aDepartment of Engineering Design, Indian Institute of Technology Madras, Tamilnadu-600036, India

^bDepartment of Electrical Engineering, Indian Institute of Technology Madras, Tamilnadu-600036, India

*Corresponding author: sathieesh@gmail.com

Article history

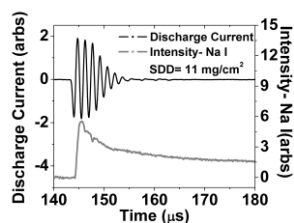
Received :15 February 2013

Received in revised form :

10 June 2013

Accepted :16 July 2013

Graphical abstract



Abstract

Lightning damage to offshore wind turbine power plants require an immediate attention, due to its severe damage to wind blade causing outage for a long time. The risk of lightning striking the blade is expected to be higher when they are located in a highly polluted and humid zone. Sodium chloride (NaCl) is considered to be among the severe pollutant near sea transported through air and gets deposited on the blade surface thereby increasing the surface conductivity of the material. Lightning can strike any part of the blade other than the receptors and the polluted surface with higher conductivity can allow discharge current to propagate over the surface thus causing severe burning of material and damaging the blade. Hence it is necessary to study the influence of salt deposit on a wind turbine blade injected with standard lightning impulse and switching impulse voltages. Wave profile and polarity has an effect during discharge because of its unique discharge formation process. Preliminary experiments are carried out in laboratory to study the influence of salt deposit on a blade sample by adopting IEC 60507 standards. Experimental results clearly show the extent of surface damage increases with increase in salt concentration. Optical emission based non-intrusive technique is used for an elemental analysis during the discharge process. Optical Emission Spectroscopy (OES) studies clearly show switching impulse voltage of both polarities induce a significant damage to the glass fiber reinforced plastic (GFRP) material.

Keywords: Lightning impulse; transient voltage; wind turbine blade; pollution; salt deposition

© 2013 Penerbit UTM Press. All rights reserved.

1.0 INTRODUCTION

The height of wind turbines with a power handling capacity of 30 kW to 7 MW lies in the range of about 200 m. A typical 7 MW wind turbine has a tower height of 160 m and a rotor diameter of 164 m (with length of blades of 70 m). Wind turbines are open air structures often placed in isolated areas where the wind condition is expected to be good, such as offshore and mountain regions. However, in such locations, due to tall structures, and sharp edges in the blade acts as a connecting point for lightning. Particularly lightning damage to a wind turbine blade is one of the major criteria causing outage and unrepairable damage of a blade material. The cost for the replacements are remarkably high and time required for the maintenance is cumbersome. Lightning protection systems such as point receptors and metallic cap receptors are placed on wind turbine blades to minimize the number of lightning strikes^{1,2} (Figure 1). Even though with this type of preventive measure, numerous lightning damages to the wind turbine blades have been reported³⁻⁶.

Summer lightning or downward initiated lightning and winter lightning or upward initiated lightning characteristics were described in literature⁷. As compared to the summer lightning, the

current duration of winter-lightning is often very long and both polarities and it tends to strike tall structures intensively. Since the energy of winter lightning is remarkably large, it causes extensive damage⁸.

Glass fiber reinforced plastics (GFRP) are used in the manufacturing of wind turbine blades as the lightning attachment probability to the blades made of all non-conductive materials is expected to be low. Further, GFRP blades also possess high mechanical strength, stiffness, smooth surface and light weight. However, in recent years the lightning damages on such non-conductive blades have also increased³⁻⁶. In offshore wind turbine power plants, most of the time the blades are subjected to sustain moisture. Soluble and non-soluble contaminants such as dust, sand and salt gets deposited on the blade surface.

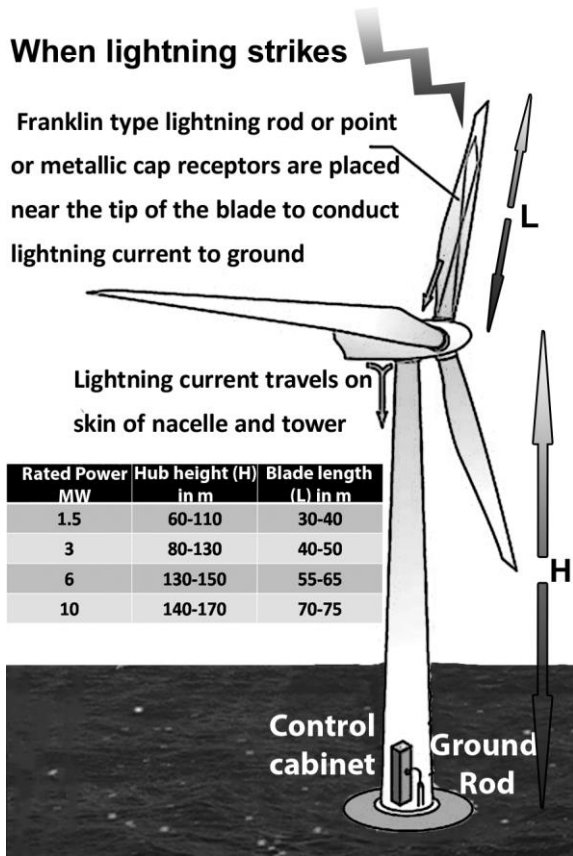


Figure 1 Offshore wind turbines with their dimensions respect to power handling capacity

Generally, surface charge accumulation and conductivity of the surface of the material increase due to the adhesion of a salt deposit. Hence lightning can strike any part of the blade other than the receptors. This is a significant problem at the electric transmission facilities around the coastal areas and similar condition was reported on outdoor insulators near coastal areas⁹. Hence for the applications of wind turbine near any offshore and near coastal areas, the influence of salt deposit or similar contaminant should be taken into consideration to avoid the wind turbine blade damage induced by lightning.

Optical emission spectroscopy (OES) technique is a non-intrusive technique to gather physical information during discharge process such as elemental analysis, plasma temperatures and density. OES technique have been used to study the plasma created during electrical discharge machining process¹⁰ and also used in measuring the characteristics of plasma generated during the wire explosion process¹¹. In this paper, an attempt have been made to study the influence of a salt deposit on a GFRP sample using OES technique during lightning discharge process from a distance of 1.5 m. The effect of pollutant with different salt deposition densities (SDD) on a GFRP material under the application of lightning impulse voltage (1.2/50 μ s similar to that of summer lightning) and switching impulse voltage (250/2500 μ s similar to that of winter lightning) of both polarities as per IEC 60507 standard is studied at laboratory level. In Sec. 2, sample preparation and experimental setup for optical emission spectroscopy technique are described. In Sec. 3, Flashover voltage, discharge current, optical emission spectra and lifetime analysis for contaminated samples on application of lightning and switching impulse voltage profiles are discussed.

2.0 EXPERIMENTAL SETUP

Experimental study was performed using woven fabric GFRP samples with surface area of 36 cm² (6 cm x 6 cm square x 3 mm thickness). Initially, NaCl with the amounts of 40 mg, 110 mg, 180 mg, 250 mg, 320 mg and 400 mg is mixed with 2100 mg of kaolin clay. Distilled water is added with the ingredients (Kaolin clay, NaCl) to form slurry and it is applied on the GFRP sample using a sprayer. The conductivity of the solution is measured using a conductivity meter (Extech instruments, pH/conductivity EC500) at a room temperature of 25° C. Equivalent salt deposition density (ESDD) and corrected conductivity (σ_{20}) of different contaminated GFRP samples are calculated as per IEC 60507 standards. Figure 2 shows corrected conductivity and ESDD corresponding to different salt concentration values.

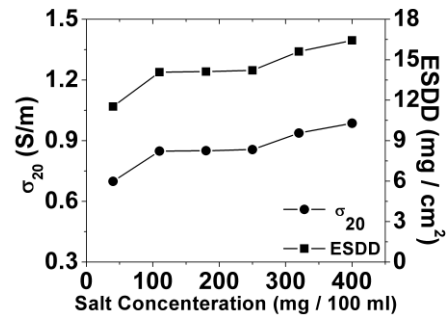


Figure 2 Determination of corrected conductivity and ESDD

Lightning impulse voltage (1.2/50 μ s) or switching impulse voltage (250/2500 μ s) of positive and negative polarity is applied to the test electrode setup which consists of two angular stainless steel electrodes tip cut for 45° (with smooth edges) placed on a GFRP sample as shown in Figure 3, 7^{12,13}.

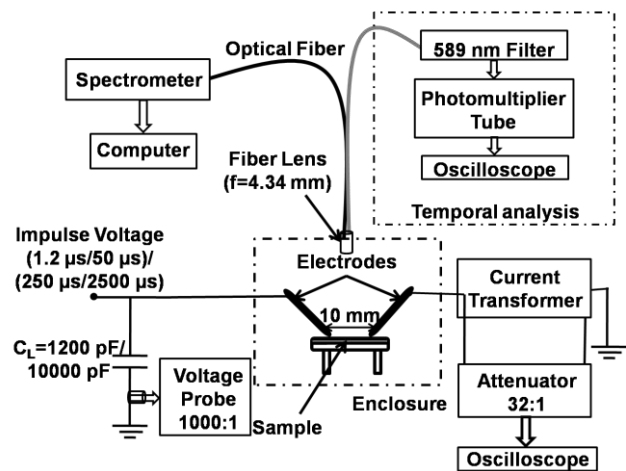


Figure 3 Optical emission spectroscopy (OES) setup

The two electrodes are separated by a gap distance of 10 mm. Applied voltage and discharge current is measured using a voltage probe (Lecroy, EP-50k, PEEC.A Japan, 1000:1) and a current probe (ETS Lindgren: Model 94111-1). Optical emission during electrical discharge on different samples is collected using a lens (focal length of 4.34 mm) combined with a multi-mode optical fiber (Core diameter of 600 μ m, Numerical aperture of

0.39). The fiber output is coupled to a spectrometer (Tech 5, Germany) with an NMOS linear image sensor (S3901, Hamamatsu). To perform neutral sodium atom (D-line, 588.99 nm) emission life time studies, Na I emission at 589 nm line was filtered using sodium filter (589 nm) and focused on to a multimode optical fiber and photomultiplier tube (R562, Hamamatsu).

3.0 RESULTS AND DISCUSSION

Glass fiber reinforced plastic (GFRP) is a polymer composite with major ingredients of silica sand (SiO₂), lime stone (CaCO₃) and soda ash (Na₂CO₃). Kaolin clay consists of 40-50% of SiO₂, 30-40% of Al₂O₃, 0-3.2% of Fe₂O₃ and 7-14% of H₂O. Determination of flashover voltage (FOV) for contaminated GFRP samples in fifteen different locations are carried out by changing the position of electrodes on the sample. The methodology to determine the FOV is described in Figure 4. The applied voltages, discharge current, rise and fall times are recorded for each flashover.

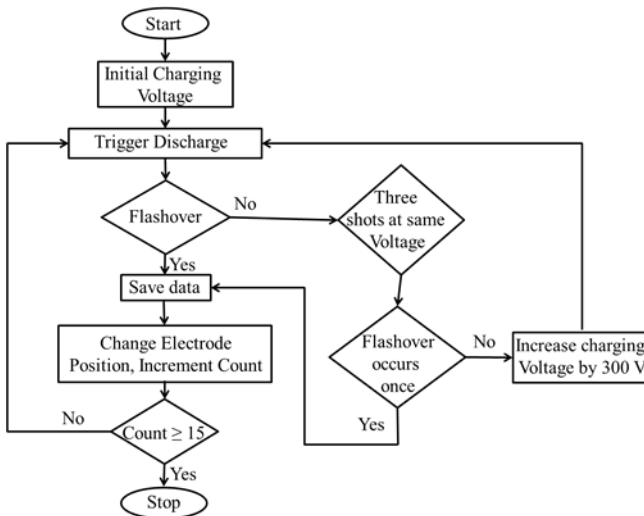


Figure 4 Flowchart to determine flashover voltage

Streamer initiation is essential as the discharge is supposed to search for the weakest link (surface defects) in the path of propagation and finally leading to a flashover. Table 1 shows experimentally observed flashover voltage for GFRP and kaolin clay deposited on GFRP sample under lightning impulse and switching impulse voltages. Flashover voltage reduces with increase in salt deposition densities for lightning impulse and switching impulse voltage (irrespective of polarity) as shown in Figures 5(a) and (b). This is due to the fact that pollutant deposited on a GFRP reduces the dielectric breakdown strength of the material and in turn expected to enhance the probability of the surface discharge phenomenon.

Table 1 Flashover voltage for an electrode gap distance of 10 mm

VOLTAGE PROFILE	GFRP (FOV in kV)	Kaolin deposited on GFRP (FOV in kV)
Positive Impulse	17.251	15.653
Negative Impulse	21.797	19.709
Positive Switching Impulse	14.186	14.040
Negative Switching Impulse	13.986	13.540

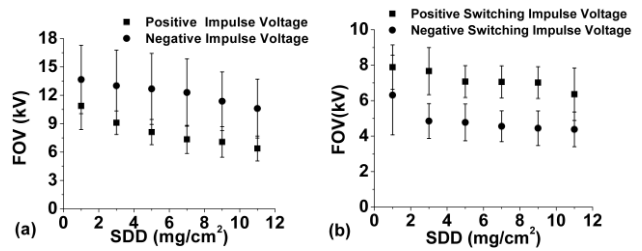


Figure 5 Flashover voltages for samples with different salt deposit density

Based on Figure 5, FOV is less under switching impulse voltage when compared with lightning impulse, irrespective of its polarity and the level of pollution. The influence of pollution on reduction in FOV is not much absurd under switching impulse voltages. Also the pollutant has a major impact under positive lightning impulse voltage when compared with negative impulse voltage.

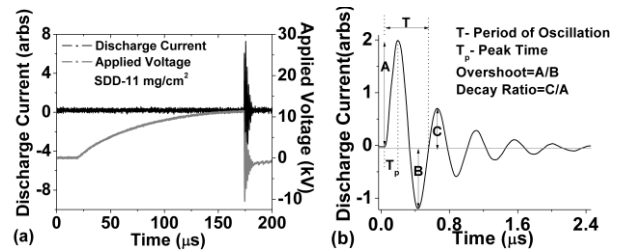


Figure 6 Applied voltage and discharge current profile during switching impulse discharge

During the initiation of the surface discharge process, the applied voltage collapses and forms a ringing pattern which leads to the ringing nature of the discharge current profile as shown in Figures 6(a) and (b) and its characteristics are summarized in Table 2.

Table 2 Characteristics of discharge current profile

PARAMETERS	IMPULSE (POSITIVE/NEGATIVE)	SWITCHING IMPULSE (POSITIVE/NEGATIVE)
Peak Time, T _p	0.16 µs	0.32 µs/ 0.75 µs
Overshoot	1.6	0.74/0.90
Decay Ratio	0.35-0.39	(0.53-0.78)/0.96
Frequency	2 MHz	750 kHz /550 kHz
Phase Angle	- 110°	+ 60°/-37°

Peak value of discharge current increased with increase in salt deposition densities during surface discharge. This was attributed to the increase in the electrical conductivity of pollutant layer due to increase in the salt deposit density. Decay ratio also increased with increase in the salt deposit density which represents a slow decay of discharge current profile and in turn sustains the temperature for a longer period. Decay ratio for negative switching impulse voltage is higher than other voltage profiles and in turn deterioration of sample occurs. Hence damage to the core material (GFRP) is severe in case of samples with higher SDD and negative switching impulse voltage as shown in Figure 7 (a-d). Figures 7(b) and (d) represents the damage induced on a sample with salt deposit density of 7 mg/cm² on application

of lightning impulse and switching impulse voltage after five successive pulses at the same electrode position on the sample.

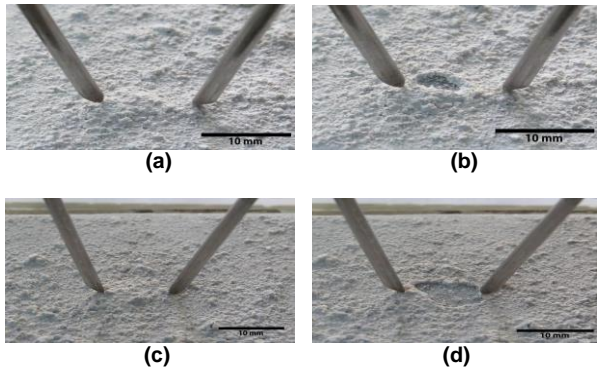


Figure 7 Damage induced on a sample with SDD= 7 mg/cm²: (a) before discharge, (b) after discharge under negative lightning impulse voltage (after 5th successive discharge at same position), (c) before discharge, (d) after discharge under negative switching impulse voltage (after 5th successive discharge at same position)

Figures 8(a), (b), (c) and (d) show optical emission spectra of GFRP, kaolin clay deposited on GFRP, sample with salt deposit density of 3 mg/cm² and 11 mg/cm². Characteristic peaks observed in the spectra relate to the elemental composition of the material¹⁴. Samples with different salt deposition densities show a significant peak at 588.99 nm which relate to a neutral sodium atom (D-line, Na I) but chlorine peaks are not observed as shown in Figure 8(c) and (d). With increase in SDD, the optical emission spectra of GFRP (underneath substrate) itself is observed representing surface damage due to electric discharge. When the discharge voltage is higher than that of the flashover voltage then the spectra of GFRP itself is observed with an addition of Na I line at 588.99 nm representing the propagation of discharge along the GFRP-Contaminant boundary.

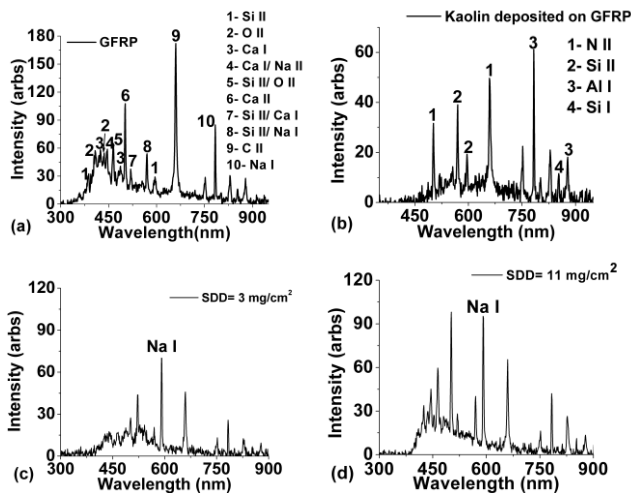


Figure 8 Typical optical emission spectra obtained during discharge. (Positive impulse voltage)

Na I emission lifetime measurements are carried out to rank the severity of pollutant deposited on a GFRP sample. Based on Figure 9 the Na I emission lifetime profile follows the discharge current profile to an extent. The life time is estimated at 20% of

the maximum emission intensity. A lifetime of 1.2 to 7.0 μs and 0.8 to 5.8 μs are observed for positive and negative impulse voltage profiles. In case of positive impulse voltage, discharge plasma emission sustained for a longer duration than negative impulse voltage.

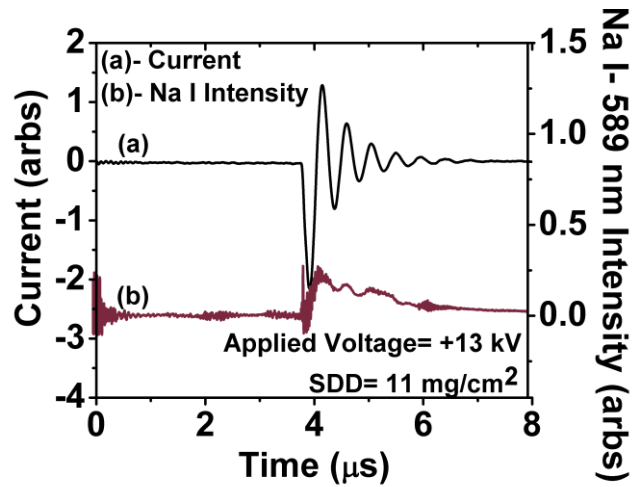


Figure 9 Typical graph indicating discharge current and Na I emission lifetime (Positive impulse voltage): (a) Discharge current, (b) Na I emission

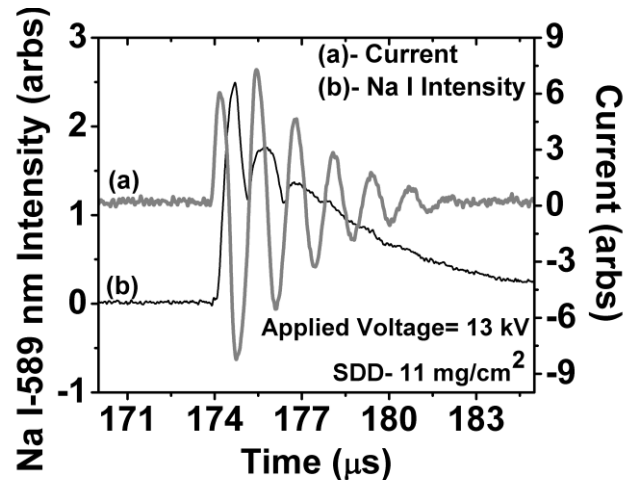


Figure 10 Typical graph indicating discharge current and Na I emission lifetime (Negative switching impulse voltage): (a) Discharge current, (b) Na I emission

Figure 10 represents the Na I emission at 589 nm profile and its relationship with discharge current for an application of negative switching impulse voltage. A Na I emission lifetime of 4 to 18 μs and 24 to 96 μs are observed for positive and negative switching impulse voltage profiles. Even though the discharge current decays fast, Na I emission in discharge plasma sustains for longer period in case of negative switching impulse voltage and enhances the deterioration of GFRP material. On an application of positive switching impulse voltage, large magnitude of current flows through the sample during surface discharge process as shown in Figure 11. This induces heating of the surface as a result of lower surface discharge impedance. Switching impulse voltage of both polarities induces a significant damage to the GFRP material compared to lightning impulse voltage. Results based on

optical emission spectroscopy studies qualitatively are in agreement with the electrical discharge measurements.

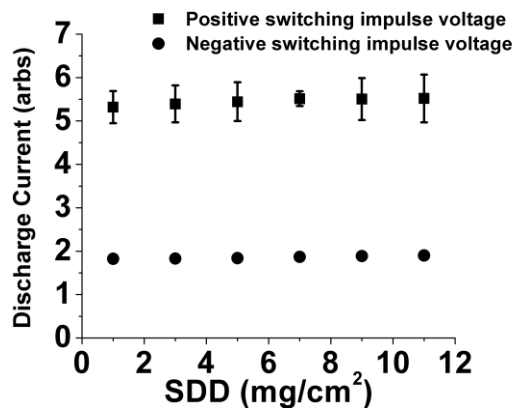


Figure 11 Discharge current measurements (Switching impulse voltage)

4.0 CONCLUSION

Optical emission spectroscopy technique is used to study the influence of salt deposit on a glass fiber reinforced plastics on applying standard lightning impulse and switching impulse voltages. Electrical discharge studies clearly show that flashover voltage decreases with increase in salt deposit density irrespective of applied voltage profiles. Lower flashover voltage is observed in case of negative switching impulse voltage as compared to other voltage profiles. Peak value of discharge current increased with increase in SDD due to increase in the electrical conductivity of the contaminated samples. Decay ratio of discharge current increased with increase in SDD and resulted in a higher value in case of negative switching impulse voltage. A slow decay of discharge current profile is expected to sustain the temperature for a long period. Hence damage to the base material (GFRP) is expected to be significant.

Optical emission spectra observed for different samples shows characteristic peaks which relates to the elemental composition of the samples. Na I emission line at 588.99 nm could be identified for samples with different contamination level. With increase in SDD, the optical emission spectra of GFRP (underneath substrate) itself is observed representing surface damage leading to carbonization. Na I emission in discharge plasma sustains for longer period in case of negative switching impulse voltage and enhances the deterioration of GFRP material.

Large magnitude of current flows through the sample during surface discharge process on application of positive switching impulse voltage which represents low discharge impedance and hence heating of surface is pronounced. Switching impulse voltage of both polarities induce a significant damage to the GFRP material. Results based on optical emission spectroscopy studies qualitatively are in agreement with the electrical discharge measurements. Hence OES technique can be used to understand the discharge mechanism and the extent of material damage occurrence during lightning discharge process.

Acknowledgement

This work is financially supported by Department of Science and Technology (SR/S3/EECE/0115/2010).

References

- [1] I. Cotton, B. McNiff, T. Soerenson, W. Zischank, P. Christiansen, M. Hoppe-Kippler, S. Ramakers, P. Pettersson, E. Muljadi. 2000. *International Conf. Lightning Protection (ICLP)*. 848.
- [2] S. F. Madsen, F. M. Larsen, L. B. Hansen, K. Bertelsen. 2004. *IEEE Intern. Symp. Electrical Insulation (ISEI)*. 484.
- [3] T. Naka, N. J. Vasa, S. Yokoyama, A. Wada, S. Arinaga. 2006. *Intern. Conf. Lightning Protection (ICLP)*. 11a2.
- [4] N. J. Vasa, T. Naka, S. Yokoyama, A. Wada, A. Asakawa. 2006. *Intern. Conf. Lightning Protection (ICLP)*. 11a1.
- [5] S. Sekioka, K. Yamamoto, M. Minowa, S. Yokoyama. 2007. *IX Intern. Symp. Lightning Protection*.
- [6] T. Naka, N. J. Vasa, S. Yokoyama, A. Wada, A. Asakawa, H. Honda, K. Tsutsumi, S. Arinaga. 2005. *IEEE Trans. Power Engineering*. 125: 993.
- [7] V. A. Rakov, M. A. Uman. 2003. *Lightning-Physics and Effects*. New York: Cambridge University Press.
- [8] K. Miyake, T. Suzuki, K. Shinjou. 1992. *IEEE Trans. on Power Delivery*. 7: 1450.
- [9] M. A. Douar, A. Mekhaldi, M. C. Bouzidi. 2010. *IEEE Trans. Dielectrics and Electrical Insulation*. 17: 1284.
- [10] A. Descoedres, Ch. Hollenstein, R. Demellayer, G. Walder. 2004. *J. Physics D, Applied Physics*. 37: 875.
- [11] Jobin K. Antony, Nilesh J. Vasa, S. R. Chakravarthy, R. Sarathi. 2010. *J. Quantitative Spectroscopy and Radiative Transfer*. 111: 2509.
- [12] R. Sarathi, G. Nagesh, K. Vasudevan. 2008. *World Academy of Science, Engineering and Technology*. 15: 177.
- [13] V. Sathiesh Kumar, Nilesh J. Vasa, R. Sarathi. 2012. *J. Applied Physics A*. Doi:10.1007/s00339-012-7219-5.
- [14] NIST Handbook of Basic Atomic Spectroscopic Data. <http://physics.nist.gov/PhyRefData/Handbook/index.html>.
- [15] Jin Xu, Zhenqian Lu. 2010. *World non grid-connected wind power and energy conference (WNWEC)*. 1.
- [16] Michael G. Danikas, R. Sarathi, P. Ramnalis, S. L. Nalmpantis. 2009. *World Academy of Science, Engineering and Technology*. 26: 871.